International Journal of Bio-Science and Bio-Technology
Vol.8, No.3 (2016), pp. 63-76
http://dx.doi.org/10.14257/ijbsbt.2016.8.3.07

Retinal Blood Vessel Segmentation Algorithms: A Comparative Survey

Meenu Garg and Sheifali Gupta

School of Electronics and Electrical Engineering,
Chitkara University, Chandigarh, India
meenu.garg@chitkara.edu.in, sheifali.gupta@chitkara.edu.in

Abstract

Automated segmentation and delineation of morphological properties of retinal vascular network had now become the most important research area in the treatment of ophthalmologic disorders. With the advancement of computational efficiency, image processing methodologies are widely used in ophthalmology. This paper gives the review of various segmentation techniques implemented by various authors in conjunction with performance metrics like sensitivity, specificity, accuracy and area under the curve. Results of various algorithms has been compared and analyzed. For the extraction of retinal vasculature, 2D retinal image from various databases has been considered.

***Keywords**: Retinal blood vessel; Segmentation; Methodologies; Database; Performance metrics;*

1. Introduction

In the fundus image of retina, retinal vasculature is a complex network, which consists of hollow pipes of various dimensions. Retinal vascular network includes arteries, arterioles, capillaries, veins and venules. Arteries are brighter and they are used to transport blood high in oxygen level to the various organs of the body and the veins are darker and they are used to transport blood low in oxygen level.

Information about location of the retinal vasculature, assessment of its morphological attributes like length, diameter, width, tortuosity and branching angle and detection of abnormalities is important for diagnosis, screening and treatment of various disorders such as stroke, cardiovascular diseases, hypertension, diabetes and arteriosclerosis. This tree-like structure is also useful to find the other normal features of retina such as macula or fovea or optic disk or for the automatic identification of pathological elements like hemorrhage, micro aneurysms, exudates or lesions.

Vascular diseases present a challenging health problem for society. So, superior image segmentation algorithms are needed for understanding and management of these circumstances in a better way.

Segmentation of vessels in an accurate manner is a tedious job because of the following reasons:

- Less variations in the contrast between vasculature and surrounding tissue
- Presence of noise in the retina image
- Variation in the vessel width, branching angle, brightness, and shape.
- Presence of exudates, lesions, hemorrhage and other pathologies.

Segmentation of vessels is possible using manual segmentation methods, semi-automatic methods and fully automatic methods. Segmentation of blood vessels using manual method and semi-automatic method is very tedious and time consuming task because high skills and training is required in both these methods. Moreover these segmentation techniques are susceptible to errors. With the use of fully automatic segmentation techniques problem of manual segmentation and semi-automatic segmentation can be overcome. These automatic techniques are helpful in the advancement of computer-aided diagnostic systems which are used for diagnosis of ophthalmic disorders. Several algorithms and techniques by various authors have been presented in this paper. The main goal of the paper is to compare various image processing techniques and to analyze various performance metrics obtained after automatic segmentation of retinal vessels. Figure 1 represents structures like arteries, veins, fovea, optic disc and various pathologies present in retinal images.

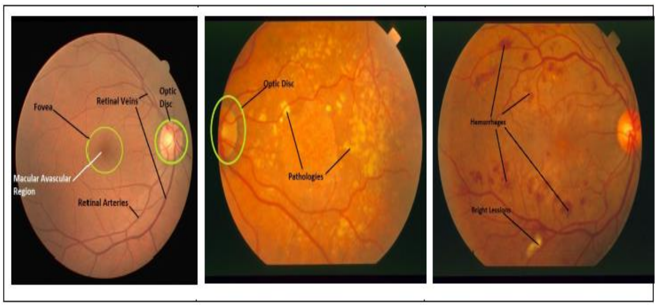

Figure 1. Anatomical Structures in Retinal Images [1]

The remaining paper includes the following sections: Section II describes the information about image databases and performance metrics used in blood vessel segmentation techniques. Section III presents classification of various retinal image segmentation techniques and brief description of each technique. Section IV illustrates the conclusion and future scope.

2. Database and Performance Metrics

A. Database

Retinal databases are those which contain normal and pathological images. Database in conjunction with type of images, field of view and size are represented in Table 1.

Table 1. Details of Database Used

Database	Year	Retinal images	FOV(Field of view) and image size
DRIVE [2] (Digital Retinal Images for Vessel Extraction)	2000	40 color fundus photographs: 20 test and 20 training images; 7 are pathological and rest are normal	45^0 768 X 584
STARE [3] (Structural Analysis of Retina)	2000	20 images: 10 are pathological and 10 are normal	35^0 650 X 500
ARIA (Automated Retinal Image Analysis) online	2006	92 images with age-related macular degeneration (AMD): 59 images with diabetes and a61 images in control group	50^0 768 X 576
ImageRet	2008	DIARETDB0 (Diabetic Retinopathy Database): 130 retinal images in which 20 are normal and 110 with diabetic retinopathy (DR). DIARETDB1 contains 89 images out of which 5 images are normal and 84 have proliferative DR.	50^0 1500 X 1152
Messidor	2008	1200 images with pathologies. 800 images with pupil dilation	45^0 1440 X 960, 2240 X 1488 2304 X 1536
ROC microaneurysm set	2009	100 digital color fundus photographs containing microaneurysms: 50 training and 50 test images.	45^0 768 X 576 1058 X 1061 1389 X 1383 768 X 584

B. Performance Metrics

Pixel base classification is used for extraction of blood vessels from the fundus image. Pixel classification is done on the basis of whether the pixel belongs to vessel or surrounding tissue. So, four different possible events are possible which include pixel classifications and pixel misclassifications. True positive (TP) and true negative (TN) are the two pixel classifications and false positive (FP), and false negative (FN) are the two pixel misclassifications. Number of these four different classifications can be used for evaluation of various performance metrics.

An event is classified as TP if a vessel pixel is correctly identified as vessel and TN if the non-vessel pixel or pixel in the surrounding tissue is correctly identified as non-vessel pixel.

An event is said to be FN if the predicted pixel represents non-vessel pixel but actually it was vessel pixel. An event is said to be FP if the predicted pixel represents vessel pixel but actually it was non-vessel pixel.

The important performance metrics which can be derived from the above events are given below:

1) TPR:

TPR can be defined as the proportion of pixels correctly detected as vessel pixels. The ratio of number of pixels correctly identified as vessel pixel to the number of pixels present actually in vessel area can be used for evaluation of TPR.

$$\mathrm{TPR} = \frac{\mathrm{TP}}{\mathrm{TP} + \mathrm{FN}}$$

2) TNR: The ratio of number of pixels correctly identified as non vessel pixel to the number of pixels present actually in non vessel area can be used for evaluation of TNR.

$$\mathrm{TNR} = \frac{\mathrm{TN}}{\mathrm{TN} + \mathrm{FP}}$$

3) FPR:

FPR can be defined as the proportion of pixels incorrectly identified as vessel pixels. The ratio of number of pixels erroneously identified as vessel pixels to the number of pixels present actually in non-vessel area can be used for evaluation of FPR

$$\mathrm{FPR} = \frac{\mathrm{FP}}{\mathrm{TN} + \mathrm{FP}}$$

FPR can also be expressed as, FPR = 1 – TNR.

4) FNR:

The ratio of number of pixels erroneously identified as non vessel pixels to the number of pixels present actually in vessel area can be used for evaluation of FNR

$$\mathrm{FNR} = \frac{\mathrm{FN}}{\mathrm{TP} + \mathrm{FN}}$$

FNR can also be expressed as, FNR = 1 – TPR.

5) Accuracy (Acc):

Acc is evaluated by taking the ratio of total number of true events which is the sum of TP and TN, to the total population which is the total number of pixels actually present in the image. The formula for accuracy is

$$\mathrm{Acc} = \frac{\sum \mathrm{TP} + \sum \mathrm{TN}}{\sum \text{Total Population}}$$

6) Sensitivity (SN):

SN metrics represents the ability of a segmentation method to detect the vessel pixels. SN is defined as the ratio of TP to the sum of TP and FN. Range of sensitivity is between 0 and 1. More SN means algorithm is able to identify vessel pixels correctly. SN measure is expressed as

$$\text{Sensitivity} = \frac{TP}{(TP + FN)}$$

SN can also be expressed as SN= 1- FNR.

7) Specificity (SP):

SP metrics represents the ability of a segmentation algorithm to detect background or non-vessel pixels. SP is also defined as the ratio of TN to the sum of TN and FP. Range of specificity is also between 0 and 1. More SP means algorithm is able to identify non-vessel pixels correctly. SP measures is expressed as

$$\text{Specificity} = \frac{TN}{(TN + FP)}$$

SP can also be expressed as, SP = 1 – FPR

8) Area under curve (AUC):

Receiver operating characteristic (ROC) curve is used to extract AUC that is widely used performance metrics. A ROC curve is the curve which plots the graph between 1-SP versus SN. The value of AUC should be 1 for optimal systems. The performance of the system is better, if the curve approaches closer to the top left corner. In case of retinal images, pixels inside the field of view (FOV) are considered for computation of TPR and FPR.

3. Classification of Various Vessel Segmentation Algorithms

In this paper, various vessel segmentation techniques are categorized according to the methodologies employed in image processing. Image segmentation algorithms are mainly classified into following categories; some of them are further classified. Various segmentation techniques used for extraction of blood vessels are supervised methods, unsupervised methods, matched filtering approach, morphological approach and deformable models. Several retinal blood vessel segmentation techniques proposed by [4]-[28] are encapsulated in this category.

A. Supervised Classification:

Supervised classification techniques require some labels to judge whether a particular pixel belongs to a vessel or surrounding tissue. So, in historical data, right answers are present in labels. Labeled training data is used by supervised segmentation methods for the training of the classifier. These classifiers can be used to classify pixels either as vessel or non-vessel in a new field of view. Various classifiers used in segmentation are artificial neural networks (ANN), support vector machine (SVM), k-nearest neighbors, AdaBoost, Gaussian mixture models (GMM)). An advantage of supervised classification is that accuracy of system is more due to presence of labeled data. But the disadvantage is that it requires human effort in the loop.

B. Unsupervised Classification:

Unsupervised methods do not require any prior labeling information for the segmentation of retinal vasculature from fundus image. So, in historical records, no wrong or right answers are present. Intrinsic patterns of vessels can be find out using unsupervised classification methods which can be further used for classification of pixels. An advantage of unsupervised classification is that it requires minimal human effort in the loop. But the disadvantage is that accuracy of system is less due to absence of labeled data,.

C. Matched Filter:

Matched filters approach convolve a 2-D structural element (kernel) which is linear in nature with a retinal image for segmentation and detection of retinal vascular network. The kernel is designed to rotate at many different orientations to fit into vessels of various configurations and presence of this feature is identified by the matched filter response (MFR). Due to the less contrast variation between vessel and surrounding tissue or due to the presence of noise and pathologies in the fundus image, number of false responses increase. So, MFR method in conjunction with various image processing techniques is found to be very efficient. Image enhancement is performed with the help of matched filters which do not perform in isolation, so this approach is followed by other approaches like thresholding for the correct identification of pixels belongs to vessel.

D. Morphological Operations:

The word morphology deals with the shape and structures of objects. Several techniques used in digital image processing are based on mathematical morphology. Two operators used in morphological processing are Dilation and Erosion. Structuring elements (SE) of certain intensity and shape is used by the dilation and erosion operations. Expansion of object is dome by dilation operator and compression of object id done by erosion operator. Two more operations are opening and closing of an image which is built up from dilation and erosion.

Opening operation on image I using the structuring element S is defined by the following mathematical expression.

$$I \circ S = (I \ominus S) \oplus S$$

Closing operation on image I using the structuring element S is defined by the following mathematical expression.

$$I.S = (I \oplus S) \ominus S$$

Where $\oplus$ represents dilation operation and $\ominus$ represents erosion operation.

Opening and closing operations are mostly used together in various morphological operations used in image segmentation process for the selection of features. Features size can be enlarged and reduced repeatedly with the help of these operations, allowing the elimination of noise and very small details. Watershed and top hat transformations are the two methodologies which are related to the mathematical morphology and can be used in image segmentation for numerous medical applications.

E. Deformable models

Deformable models are used for segmentation to search out the proper shape or boundary of the object by using initial contour. These deformable models are further classified into two main categories: Parametric deformable models (PDM) and Geometric Deformable Models (GDM).

1) Parametric deformable models (PDM):

Active contours models or snakes are used to locate the boundary of the object or extract the important feature from the fundus image by using the initial contour. Parametric curve is used for the modeling of active contour and this curve tries to find the minimum energy by moving the points of the contour to its minimum neighborhood. The energy of the snake is computed form internal and external energy, so the sum of both these energies is minimized to get minimum snake energy.

The snake energy is the combination of three terms: E_{int} ,E_{img} , E_{con}. E_{int} represents the internal energy of the snake, E_{img} represents the energy of the image and the E_{con} represents the energy of the external constraint forces.

Mathematically the internal energy of the snake is shown as

$$E_{int} = \frac{1}{2}\left(\alpha(s)\|v_s(s)\|^2 + \beta(s)\|v_{ss}(s)\|^2\right)$$

where alpha(α) and beta (β) are the two coefficients used for controlling the energy of the snake. v(s) represents the position of snake given by the curve where $s \epsilon [0,1]$.

$\|v_s(s)\|^2$ and $\|v_{ss}(s)\|^2$) represents measure of elasticity and curvature respectively. ,E_{img} is computed by taking the gradient of image. Sometimes Gaussian filter is applied to the image for the removal of noise, if present. After that gradients are evaluated to find the energy of the image.

Mathematically image energy with 2D Gaussian filter can be expressed as

$$E_{img} = \|\nabla\,[(G(x,y) * I(x,y))]\|^2$$

Sign of image energy may be different for different algorithms used for extraction of vessels.

As compared to other classical feature extraction techniques, active contour models have many advantages:

- Minimum state is searched adaptively and autonomously.
- Sensitivity is introduced with the use of Gaussian smoothing in the image energy function
- Dynamic objects can be tracked.

Along with the advantages, these models also possess some key drawbacks.

- Active contour models are sensitive to local minima states, but with the use of simulated annealing techniques this effect can be counteracted.
- During energy minimization, minute features are ignored over the entire contour.

2) Geometric deformable models

GDM are used to tackle the limitations present in PDM: they are independent of parameterization; no self-intersections are produced because they are numerically stable and topology changes can be permitted automatically. Level set techniques and curve evolution theory is the base of GDM. These surfaces and curves are evolved using geometric measures only, leading to a contour evolution that does not depend on parameterization and can be represented implicitly.

Comparison of various algorithms, image processing techniques and performance metrics (SN, SP, ACC, AUC) proposed by different authors is shown in Table 2.

Table 2. Comparison of Various Performance Metrics

Reference	Year	Author	Image Segmentation Technique	Database	Performance metrics			
					SN	*SP*	*ACC*	*AUC*
[4]	1989	Chaudhuri et al.	2D Gaussian matched filter has been used for image segmentation	DRIVE	_	_	0.8773	0.7878
[5]	2004	Staal et al.	Image ridges are used for segmentation and k-NN classifiers are used for classification of feature vectors.	DRIVE STARE	_ _	_ _	0.9442 0.9516	0.952 0.9614
[6]	2006	Soares et al.	Morlet wavelet has been used for filtering of noise and enhancement of vessels. After that GMM classifier has been used on enhanced image for further classification of pixels.	DRIVE STARE	_ _	_ _	0.9466 0.9480	0.9614 0.9671
[7]	2007	Mendonca and Campilho	Initially vessel centerlines are detected and then Multiscale morphological reconstruction is used for image segmentation	DRIVE STARE	0.7344 0.6996	0.9764 0.9730	0.9452 0.9440	_ _
[8]	2007	Ricci and Perffetti	Line operator is used for the construction of feature vector which is further used for supervised classification using Support Vector Machine (SVM) .	DRIVE STARE	_ _	_ _	0.9563 0.9584	0.9558 0.9602
[9]	2007	Li et al	Multiresoution Hermite model has been used for analysis of retinal vasculature.	DRIVE STARE	0.780 0.752	0.978 0.980	_ _	_ _
[10]	2008	Alonso-Montes et al.	Pixel level snakes (PLS) has been used for extraction and testing of retinal vessel tree. Execution time and accuracy has also been analysed.	DRIVE	_ _	_ _	0.9185	0.9011
[11]	2008	Perfetti et al	Cellular neural network (CNN) has been used for extraction of vessels.	DRIVE			0.9261	0.9348
[12]	2009	Al-Diri et al	Ribbon of Twin (ROT) active contour model has been used for image segmentation	DRIVE STARE	0.7282 0.7521	0.9551 0.9681	_ _	_ _
[13]	2009	Osareh et al	Fuzzy c-means clustering has been used for the segmentation of colored image. Features such as color, size, edge strength, and texture are extracted and then multilayer neural network	DRIVE(SV M) DRIVE(G	0.9650 0.9614	0.9710 0.9484	0.9675 0.9524	0.974 0.965

			classifier has been used for the classiification of feature vector.	MM)				
[14]	2010	Lam et al	Multiconcavity modeling has been used for image segmentation	DRIVE STARE	_ _	_ _	0.9472 0.9567	0.9614 0.9739
[15]	2010	Lupascu et al	AdaBoost classifier has been used for classification of pixels.	DRIVE	0.72	_	0.9597	0.9561
[16]	2010	Palomera-Perez et al	ITK parallel implementation has been used for image segmentation.A huge amount of high-resolution retinal images has been anlyzed using this approach.	DRIVE STARE	0.64 0.769	0.967 0.9449	0.9250 0.926	_ _
[17]	2011	Marin et al	Gray level and moment invariant based features with neural network have been used for pixel representation.	DRIVE STARE	0.7067 0.6944	0.9801 0.9819	0.9452 0.9526	0.9588 0.9769
[18]	2012	Akram et al	2-D Gabor wavelet has been used for enhancement and multilayered thresholding technique has been used for vessel segmentation.	DRIVE STARE	_ _	_ _	0.9469 0.9502	0.9632 0.9706
[19]	2012	Bankhead et al	Wavelets has been used for the extraction of blood vessel network.	DRIVE STARE	0.703 0.758	0.971 0.950	0.9371 0.932	0.837 0.854
[20]	2012	Fraz et al	Ensemble system of bagged and boosted decision trees has been used .	DRIVE STARE CHASE_DB1	0.7406 0.7548 0.7224	0.9807 0.9763 0.9711	0.9480 0.9534 0.9469	0.9747 0.9768 0.9712
[21]	2012	Saghapour et al	An active contour model has been used for extraction of vasculature from retinal fundus image.	DRIVE	0.7453	0.9481	0.9380	
[20]	2013	Wang et al	Matched filtering with multiwavelet kernels has been used for vessel enhancement. Multiscale hierarchical decomposition is used for removal of noise and localization of vessels . Finally , the vasculature is obtained by locally adaptive thresholding.	DRIVE STARE	_ _	_ _	0.9461 0.9521	0.9543 0.9682
[21]	2013	Yin et al	Probabilistic tracking-based method has been used for image segmentation	DRIVE STARE	0.6522 0.7248	0.9710 0.9666	_ _	_ _
[22]	2014	Ravichandran et al	Local entropy based thresholding technique has been used for image segmentation	DRIVE STARE	0.7259 0.7693	0.9799 0.7693	0.9574 0.9526	_ _
	2014	Shuangling Wang et al	Combination of two superiorclassifiers: ConvolutionalNeuralNetwork(CNN) andRandomForest(RF) has been used for classification	DRIVE STARE	0.8173 0.8104	0.9733 0.9791	0.9767 0.9813	0.9475 0.9751
[23]	2015	Roychowdhury	Major vessels are detected firstly and then Gaussian mixture model (GMM) classifier has been used to classify remaining pixels.	DRIVE STARE	0.725 0.772	0.983 0.973	0.952 0.951	0.962 0.969
[24]	2015	Zhao et al	The active contour method based on graph cut approach is used for segmentation of the vessels from the enhanced images obtained after the local phase filter.	DRIVE STARE ARIA VAMPIRE	0.744 0.786 0.751 0.721	0.978 0.975 0.930 0.984	0.953 0.951 0.940 0.976	0.861 0.881 0.841 0.853
[25]	2015	Zhao et al	New infinite active contour model has been used for automated detection of retinal blood vessels.	DRIVE STARE	0.742 0.780	0.982 0.978	0.954 0.956	0.862 0.874

4. Discussion

On the basis of literature survey as mentioned in the Table II, various plots for performance metrics is drawn for DRIVE and STARE databases. Table III represents SN and SP for DRIVE database calculated by various authors & Fig 2 represents the graph for the same. Table IV represents Acc and AUC for DRIVE database and Fig 3 represent the graph for the same. Table V represents SN and SP for STARE database calculated by various authors. Fig 4 represents the graph for the same. Table VI represents Acc and AUC for DRIVE database and Fig 5 represent the graph for the same.

Table 3. Sensitivity and Specificity for DRIVE database

Author Name	SN	SP
Mendonca et al (2007)	0.7344	0.9764
Li et al (2007)	0.7800	0.9780
Al-Diri et al (2009)	0.7282	0.9551
Osareh et al (2009)	0.9650	0.9710
Palomera-Perez et al (2010)	0.6400	0.9670
Marin et al (2011)	0.7067	0.9801
Bankhead et al (2012)	0.7030	0.9710
Fraz et al (2012)	0.7406	0.9807
Saghapour et al (2012)	0.7453	0.9481
Yin et al (2013)	0.6522	0.9710
Wang et al (2014)	0.8173	0.9733
Ravichandran et al (2014)	0.7259	0.9799
Roychowdhury (2015)	0.7250	0.9830
Zhao et al (2015)	0.7440	0.9780
Zhao et al (2015)	0.7420	0.9820

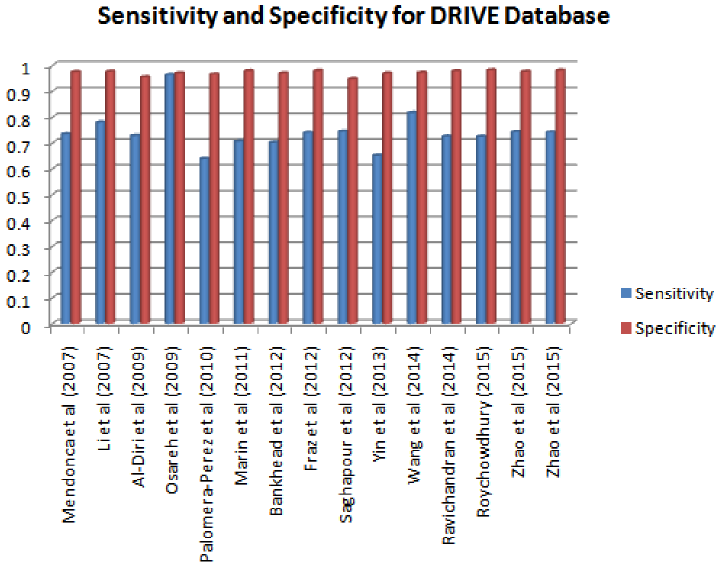

Figure 2. Sensitivity and Specificity for DRIVE Database

Table 4. Acc and AUC for DRIVE Database

Author Name	ACC	AUC
Chaudhuri et al. (1989)	0.8773	0.7878
Staal et al. (2004)	0.9442	0.952
Soares et al. (2006)	0.9466	0.9614
Ricci and Perffetti (2007)	0.9563	0.9558
Alonso-Montes et al. (2008)	0.9185	0.9011
Perfetti et al (2008)	0.9261	0.9348
Osareh et al (2009)	0.9675	0.974
Lam et al (2010)	0.9472	0.9614
Lupascu et al (2010)	0.9597	0.9561
Marin et al (2011)	0.9452	0.9588
Akram et al (2012)	0.9469	0.9632
Bankhead et al (2012)	0.9371	0.837
Fraz et al (2012)	0.948	0.9747
Wang et al (2013)	0.9461	0.9543
Wang et al (2014)	0.9767	0.9475
Roychowdhury (2015)	0.952	0.962
Zhao et al (2015)	0.953	0.861
Zhao et al (2015)	0.954	0.862

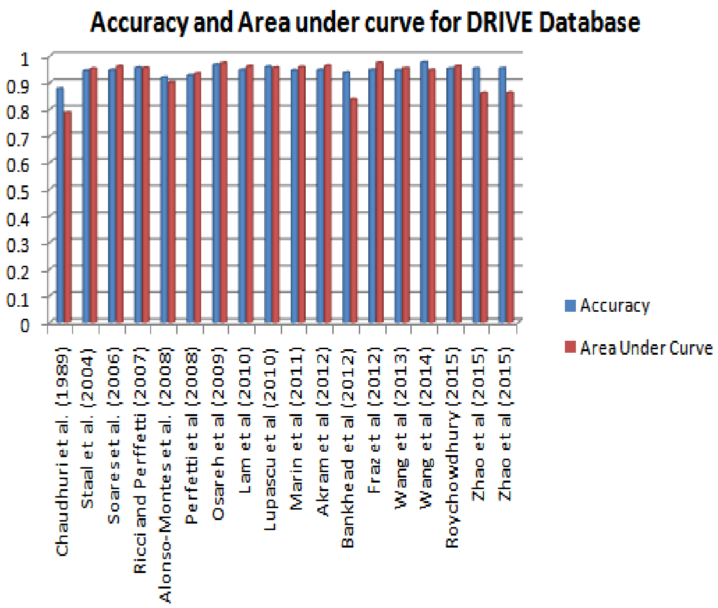

Figure 3. Acc and AUC for DRIVE Database

Table 5. SN and SP for STARE Database

Author Name	SN	SP
Mendonca et al (2007)	0.6996	0.973
Li et al (2007)	0.752	0.98
Al-Diri et al (2009)	0.7521	0.9681
Perez et al (2010)	0.769	0.9449
Marin et al (2011)	0.6944	0.9819
Bankhead et al (2012)	0.758	0.95
Fraz et al (2012)	0.7548	0.9763
Yin et al (2013)	0.7248	0.9666
Wang et al (2014)	0.8104	0.9791
Ravichandran et al (2014)	0.7693	0.7693
Roychowdhury (2015)	0.772	0.973
Zhao et al (2015)	0.786	0.975
Zhao et al (2015)	0.78	0.978

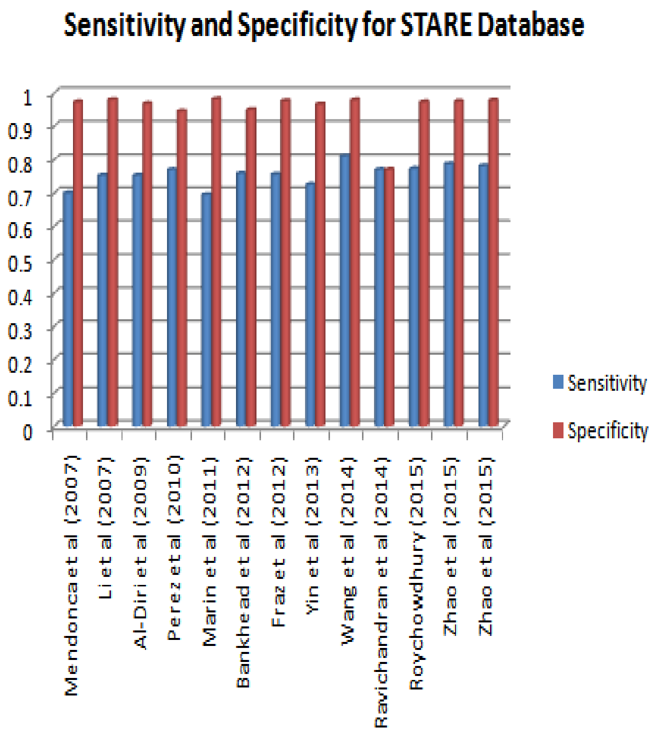

Figure 4. Sensitivity and Specificity for STARE Database

Table 6. Acc and AUC for STARE Database

Author Name	ACC	AUC
Staal et al. (2004)	0.9516	0.9614
Soares et al. (2006)	0.948	0.9671
Ricci et al (2007)	0.9584	0.9602
Lam et al (2010)	0.9567	0.9739
Marin et al (2011)	0.9526	0.9769
Akram et al (2012)	0.9502	0.9706
Bankhead et al (2012)	0.932	0.854
Fraz et al (2012)	0.9534	0.9768
Wang et al (2013)	0.9521	0.9682
Wang et al (2014)	0.9813	0.9751
Roychowdhury (2015)	0.951	0.969
Zhao et al (2015)	0.951	0.881
Zhao et al (2015)	0.956	0.874

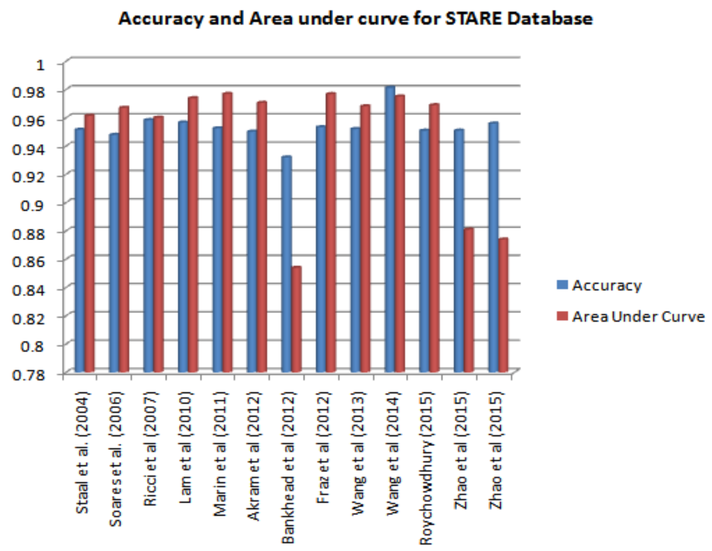

Figure 5. Acc and AUC for STARE Database

5. Conclusion

In recent years, the extraction of the vasculature from the intricate network becomes a major research area. The correct extraction of the retinal vasculature is necessary for screening and identification of ophthalmologic disorders. The main motive of this paper is to introduce various retinal segmentation techniques in conjunction with the performance metrics like SN, SP, Acc and AUC for various databases, found in literature. Although many promising retinal vessel segmentation techniques are developed but still there is a scope for improvement in vessel segmentation methodologies because the future direction of segmentation analysis are going to be towards developing automated, quicker and accurate techniques.

References

[1] James, Edward, and A. Francisco, "On Supervised Methods for Segmentation of Blood Vessels in Ocular Fundus Images", Advances in Image and Video Processing, vol. 1, no. 1, **(2013)**.
[2] http://www.isi.uu.nl/Research/Datasets/DRIVE/
[3] http://www.ces.clemson.edu/_ahoover/stare/
[4] S. Chaudhuri, S. Chatterjee, N. Katz, M. Nelson and M. Goldbaum, "Detection of blood vessels in retinal images using two-dimensional matched filters", IEEE Trans. Med. Imag., vol. 25, **(1989)**, pp. 203–210.
[5] J. Staal, M. Abramoff, M. Niemeijer, M. Viergever and B. V. Ginneken, "Ridge-based vessel segmentation in color images of the retina", IEEE Trans. Med. Imag., vol. 23, **(2004)**, pp. 501–509.
[6] J. Soares and M. Cree, "Retinal vessel segmentation using the 2D Gabor wavelet and supervised classification", IEEE Trans. Med. Imag., vol. 25, **(2006)**, pp. 1214–1222.
[7] A. Mendonca and A. C. Campilho, "Segmentation of retinal blood vessels by combining the detection of centerlines and morphological reconstruction", IEEE Trans. Med. Imag., vol. 25, **(2007)**, pp. 1200–1213.
[8] Ricci and R. Perfetti, "Retinal blood vessel segmentation using line operators and support vector classification", IEEE Trans. Med. Imag., vol. 26, **(2007)**, pp. 1357–1365.
[9] W. Li, A. Bhalerao and R. Wilson, "Analysis of retinal vasculature using a multiresolution Hermite model", IEEE Transactions on Medical Imaging, vol. 26, **(2007)**, pp. 137–152.
[10] C. A. Montes, D. L. Vilario, P. Dudek and M. G. Penedo, "Fast retinal vessel tree extraction: a pixel parallel approach", International Journal of Circuit Theory and Applications, vol. 36, **(2008)**, pp. 641–651.
[11] R. Perfetti, "Cellular neural networks with virtual template expansion for retinal vessel segmentation. Circuits and Systems II: Express Briefs", IEEE Transactions, vol. 54, no. 2, **(2007)**, pp. 141-145.
[12] B. A. Diri, A. Hunter and D. Steel, "An active contour model for segmenting and measuring retinal vessels", IEEE Transactions on Medical Imaging, vol. 28, **(2009)**, pp. 1488–1497.
[13] A. Osareh and B. Shadgar, "Automatic blood vessel segmentation in color images of retina", Iranian Journal of Science and Technology Transaction B – Engineering, vol. 33, **(2009)**, pp. 191–206.

[14] B. S. Y. Lam, G. Yongsheng and A. W. C. Liew, "General retinal vessel segmentation using regularization-based multiconcavity modeling", IEEE Transactions on Medical Imaging, vol. 29, **(2010)**, pp. 1369–1381.
[15] C. A. Lupascu, D. Tegolo and E. Trucco, "FABC: retinal vessel segmentation using AdaBoost", IEEE Transactions on Information Technology in Biomedicine, vol. 14, **(2010)**, pp. 1267–1274.
[16] M. P. Prez, M. M. Perez, H. B. Prez and J. O. Arjona, "Parallel multiscale feature extraction and region growing: application in retinal blood vessel detection", IEEE Trans. Inf. Technol. Biomed., vol. 14, **(2010)**, pp. 500–506.
[17] D. Marin, A. Aquino, M. E. G. Arias and J. M. Bravo, "A new supervised method for blood vessel segmentation in retinal images by using gray-level and moment invariants-based features", IEEE Transactions on Medical Imaging, vol. 30, **(2011)**, pp. 146–158.
[18] M. U. Akram and S. A. Khan, "Multilayered thresholding-based blood vessel segmentation for screening of diabetic retinopathy", Engineering with computers, vol. 29, no. 2, **(2013)**, pp. 165-173.
[19] P. Bankhead, "Fast retinal vessel detection and measurement using wavelets and edge location refinement", PloS one, vol. 7, no. 3, **(2012)**.
[20] M. M. Fraz, P. Remagnino, A. Hoppe, B. Uyyanonvara, A. R. Rudnicka, C. G. Owen and S. A. Barman, "Blood vessel segmentation methodologies in retinal images - a survey", Comput. Meth. Prog. Bio., vol. 108, **(2012)**, pp. 407–433.
[21] E. Saghapour and S. Zandian, "Automatic Segmentation of Retina Vessels by Using Zhang Method", Proceedings of World Academy of Science, Engineering and Technology, no. 72, World Academy of Science, Engineering and Technology (WASET), **(2012)**.
[22] Y. Wang, "Retinal vessel segmentation using multiwavelet kernels and multiscale hierarchical decomposition", Pattern Recognition, vol. 46, no. 8, **(2013)**, pp. 2117-2133.
[23] Y. Yin, A. Mouloud and S. Bourennane, "Automatic segmentation and measurement of vasculature in retinal fundus images using probabilistic formulation", Computational and mathematical methods in medicine, **(2013)**.
[24] C. G. Ravichandran and J. B. Raja, "A fast enhancement/thresholding based blood vessel segmentation for retinal image using contrast limited adaptive histogram equalization", Journal of Medical Imaging and Health Informatics, vol. 4, no. 4, **(2014)**, pp. 567-575.
[25] S. Roychowdhury, D. Koozekanani and K. Parhi, "Blood Vessel Segmentation of Fundus Images by Major Vessel Extraction and Sub-Image Classification", **(2014)**.
[26] Y. Zhao, "Retinal Vessel Segmentation: An Efficient Graph Cut Approach with Retinex and Local Phase", **(2015)**.
[27] Y. Zhao, "Automated Vessel Segmentation Using Infinite Perimeter Active Contour Model with Hybrid Region Information with Application to Retina Images", **(2015)**.